Maxwell-Bloch approach to Four-Wave Mixing in quantum dot semiconductor optical amplifiers

Niels Majer, Kathy Lüdge, and Eckehard Schöll
Institut für Theoretische Physik, Technische Univerisität Berlin, D-10623 Berlin, Germany
Email: majer@itp.tu-berlin.de

***Abstract*—We investigate the wavelength conversion efficiency of quantum dot semiconductor optical amplifiers using nondegenerate four-wave mixing. Further we calculate the linewidth enhancement factor as a function of the injection current and determine the effect of the carrier reservoir. The model is on the basis of semiconductor Maxwell-Bloch equations with microscopically calculated interband Coulomb scattering rates as input to the carrier dynamics between quantum dot ground and first excited state and quantum well.**

I. Introduction

Semiconductor devices with self-assembled quantum dots (QDs) as the gain source are experiencing an ever growing interest due to the nanoscale size of the QDs and the associated discrete nature of the energy levels. Nanolasers, single photon sources, or ultralow threshold devices can be realized using QDs. In this work we focus on the wavelength conversion properties of quantum dot semiconductor optical amplifiers (QD SOAs) using nondegenerate four-wave mixing (FWM). Small linewidth enhancement factors (α-factors) predicted and measured for quantum dot devices compared to conventional quantum well devices make them promising candidates for highly symmetric wavelength conversion. The underlying carrier dynamics, which drives the gain nonlinearities necessary for FWM to occur, is included in a detailed description of Coulomb scattering. The Coulomb scattering rates have already been successfully implemented to describe ultrafast gain recovery dynamics of QD SOAs [1] as well as laser dynamics on longer timescales without polarization dynamics with and without feedback [2]–[4] are now applied to a model with coherent QD and QW description.

II. Model

The model consists of coupled coherent optical Bloch equations for the quantum dot interband polarizations and electron- and hole occupations. The QD carriers are coupled to a 2D carrier reservoir (QW) by means of Auger scattering procecesses, which are calculated on a microscopic level via density matrix theory. The dynamical equations for the QD (QW) interband polarizations p^j_m (p_k), describing the probability of an optical transition between the respective electron and hole levels and the QD (QW) carrier occupation probabilities $f^j_{e/h,m}$ ($f^k_{e/h}$) of electrons (e) and holes (h) and the incoherent dynamics of the 2D carrier reservoir $w_{e/h}$ in slowly varying envelope and rotating wave approximation are given by the following equations

$$\frac{\partial p^j_m}{\partial t} = -i\delta\omega^j_m p^j_m - i\frac{\Omega_j}{2}\left(f^j_{e,m} + f^j_{h,m} - 1\right) - \frac{1}{T_2}p^j_m, \quad (1)$$

$$\frac{\partial f^j_{e/h,m}}{\partial t} = -\operatorname{Im}\left[\Omega_j\, p^{j\,*}_m\right] - R_{sp} + \left.\frac{\partial f^j_{e/h,m}}{\partial t}\right|_{col}, \quad (2)$$

$$\frac{\partial p_k}{\partial t} = -i\delta\omega_k p_k - i\frac{\Omega_k}{2}\left(f^e_k + f^h_k - 1\right) - \frac{1}{T_2^{QW}}p_k, \quad (3)$$

$$\frac{\partial f^k_{e/h}}{\partial t} = -\operatorname{Im}\left[\Omega_k p_k{}^*\right] + \gamma_{QW}(f^{k,eq}_{e/h} - f^k_{e/h}), \quad (4)$$

$$\frac{\partial w_{e/h}}{\partial t} = \frac{j(t)}{e_0} - \tilde{R}_{sp} - 2\sum_{m,j} N^j \left.\frac{\partial f^j_{e/h,m}}{\partial t}\right|_{col} + N\left(\frac{\partial f^k_{e/h}}{\partial t}\right). \quad (5)$$

The superscript j denotes the j-th subgroup of QDs of the inhomogeneously broadened QD ensemble with frequency detuning $\delta\omega^j_m$ with respect to the input light field. The full width at half maximum (FWHM) of the energy broadening distribution is taken to be 20 meV. The QD ground state and the first excited state are discriminated by a level index m. Scattering induced coherence loss for the QDs (QW) is accounted for by a dephasing time T_2 (T_2^{QW}). The electric current density injected into the QW is given by $j(t)$. The Rabi frequencies of the QD and QW transitions with associated dipole moments $\mu_j = 0.6\, e_0 nm$ and $\mu_k = 0.5\, e_0 nm$ enter as $\Omega_{j/k}(t) = \frac{\mu_{j/k}}{\hbar}E(t)$ in Eq. (2), respectively. Losses due to spontaneous emission in the QDs and the QW are given by R_{sp} and $\tilde{R}_{sp}$, respectively. Details can be found in [1]. The QW states $f^k_{e/h}$ relax towards quasi-equilibrium distributions $f^{k,eq}_{e/h}$ with a phenomenologically introduced relaxation rate γ_{QW}. The last term in Eq. (5) denotes the change in QW density resulting from the coherent interaction from Eq. (4). The incoherent QW contributions given by Eq. 4 lead to a change in chemical potential and thus a change in the quasi-Fermi distributions $f^{k,eq}_{e/h}$. This requires a self-consistent treatment, such that the total particle in the reservoir resulting from Eq. (4) and Eq. (5), are always equal, e.g. $\sum_k f^k_{e/h} = A w_{e/h}$, where A is the in plane area of the device. An important part of the carrier dynamics is given by the carrier scattering contributions $(\partial/\partial t) f^j_{b,m}|_{col}$ leading to a redistribution of carriers within the QW-QD system. Assuming high excitation conditions we neglect carrier-phonon collisions and restrict ourselves to Coulomb scattering processes that are calculated in a perturbation approach up to second order in the screened Coulomb potential within Markov approximation. The QD

978-1-61284-878-5/11/$26.00 ©2011 IEEE

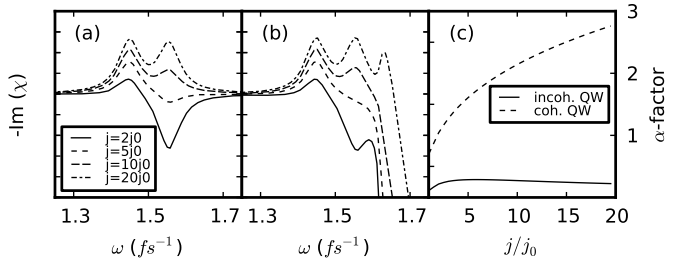

Fig. 1. (a): Linear gain spectrum in dependence of the frequency of the electric field without Eqs. (3) and (4). (b): Same as (a) for full system. (c): α-factor in dependence of the injection current. Parameters: $T_2 = 30fs$, $T_2^{QW} = 120fs$ and $\gamma_{QW} = 1/60fs^{-1}$.

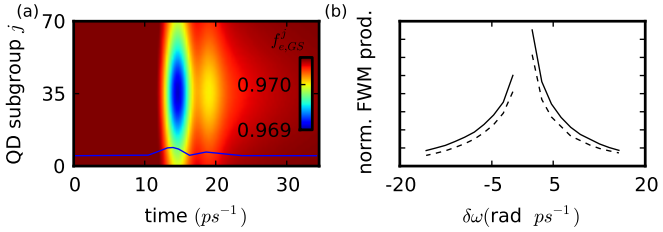

Fig. 2. (a): Density plot of the ground state (GS) QD electron occupations $f^j_{e,GS}$ versus time and subgroup index j The blue curve shows the profile of $|E(t)|$. (b): FWM product for $j = 3.2 \cdot 10^{-8} 8 e_0 nm^{-2}$ ($j \approx 10 j_0$) for the full system (black solid curves) and the reduced system (black dashed curves) in dependence of the frequency detuning of the input signals. Other parameters as in Fig 1.

ground state (GS) energy levels are adjusted to 74 meV below the QW band edge for electrons and 40 meV for holes. The excited state electron energy levels are 24 meV and hole levels 20 meV below the band edge, respectively. Details can be found in [1]. The complex slowly varying electric field amplitude $E(t)$ is taken to be a Gaussian signal with a FWHM of 5 ps in resonance to the QD ground state transition.

III. Linear gain spectra

In this section we investigate the spectral properties of the considered QD-SOA. Figure 1 (a) and (b) show plots of the gain spectra of the device for different injection currents from $j = 2j_0$ up to $j = 20j_0$ given in multiples of the transparency current j_0. In Fig. 1(a) the QW is treated incoherent, meaning that Eqs. (3) and (4) are not used in the simulation. The spectra resulting from simulations of the full system are shown in Fig. 1(b). Both figures clearly show the QD ground state transition in the lower frequency range and the QD excited state transition in the higher frequency range. In Fig 1(b) an additional gain peak originating from QW states evolves for higher injection currents. The linewidth enhancement factor, or α-factor, given in terms of the real and imaginary part of the optical susceptibility, χ' and χ'', and the total carrier density N as $\alpha(\omega) = \partial_N \chi'(\omega)/(\partial_N \chi''(\omega))$ evaluated at the QD ground state transition is shown in Fig. 1(c) in dependence of the injection current. The QD system alone, plotted as the solid curve, exhibits a much smaller α-factor than the full system. It remains below one, first increasing, then rolling over and decreasing with increasing injection currents. In case of the full system the α-factor grows in a monotonous fashion for increasing pump strength.

IV. Four-wave mixing

In this section we examine the efficiency of nondegenerate FWM in the considered QD-SOA. Two equally strong Gaussian pulses with pulse areas of $\pi/2$ and frequency detunings $\delta\omega$ are coupled into the device. The propagation of the input field within the device is calculated according to a reduced wave equation derived from Maxwell's equations [5]–[7]:

$$\left(\frac{\partial}{\partial z} + \frac{1}{\nu_g}\frac{\partial}{\partial t}\right) E(z,t) = \frac{1}{2}\Gamma i \mu_0 \frac{\omega_0 c}{n_b D} P(z,t). \qquad (6)$$

Here, $P(z,t) = 2\sum_{j,m} N^j p^j_m + \sum_k p_k$ is the macroscopic polarization, $\Gamma = 0.2$ is the optical confinement factor, μ_0 is the vacuum permeability, ω_0 is the light field frequency, c is the vacuum velocity of light, $n_b = 3.77$ is the background refractive index, and $D = 4\,nm$ is the thickness of the QW. Fig. 2(a) shows a density plot of the QD ground state electron populations $f^j_{e,GS}$ versus time and QD subgroup index j. An oscillatory behaviour required for FWM is clearly visible. In Fig. 2(b) the FWM product of the full coherent and the reduced system (cf. Fig. 1(a) and (b)) is shown. The qualitative FWM characteristic is similar in both cases .

V. Conclusion

Using a microscopically based Maxwell-Bloch approach we calculated the FWM efficiency of a QD-SOAs, the gain spectra and α-factor. While a a large contribution to the α-factor stems from the surrounding carrier reservoir the QW does not introduce significant additional asymmetries in the wavelength conversion efficiency.

Acknowledgment

This work was supported by DFG in the framework of Sfb787.

References

[1] N. Majer, K. Lüdge, and E. Schöll, "Cascading enables ultrafast gain recovery dynamics of quantum dot semiconductor optical amplifiers," *Phys. Rev. B*, vol. 82, p. 235301, 2010.

[2] K. Lüdge and E. Schöll, "Quantum-dot lasers – desynchronized nonlinear dynamics of electrons and holes," *IEEE J. Quantum Electron.*, vol. 45, no. 11, pp. 1396–1403, 2009.

[3] K. Lüdge, R. Aust, G. Fiol, M. Stubenrauch, D. Arsenijević, D. Bimberg, and E. Schöll, "Large signal response of semiconductor quantum-dot lasers," *IEEE J. Quantum Electron.*, vol. 46, no. 12, pp. 1755 –1762, 2010.

[4] C. Otto, K. Lüdge, and E. Schöll, "Modeling quantum dot lasers with optical feedback: sensitivity of bifurcation scenarios," *phys. stat. sol. (b)*, vol. 247, no. 4, p. 829, 2010.

[5] A. Knorr, R. Binder, M. Lindberg, and S. W. Koch, "Theoretical study of resonant ultrashort-pulse propagation in semiconductors," *Phys. Rev. A*, vol. 46, no. 11, pp. 7179–7186, 1992.

[6] R. Binder and S. W. Koch, "Nonequilibrium semiconductor dynamics," *Prog. Quantum Electronics*, vol. 19, no. 4-5, p. 307, 1995.

[7] J. M. M. Vazquez, H. H. Nilsson, J. Z. Zhang, and I. Galbraith, "Linewidth Enhancement Factor of Quantum-Dot Optical Amplifiers," *IEEE J. Quantum Electron.*, vol. 42, no. 10, pp. 986–993, 2006.